Resveratrol, Genistein, and Curcumin Bind Bovine Serum Albumin†

P. Bourassa,‡ C. D. Kanakis,§ P. Tarantilis,§ M. G. Pollissiou,§ and H. A. Tajmir-Riahi*,‡

Département de Chimie-Biologie, Université du Québec à Trois-Rivières, C. P. 500, Trois-Rivières (Québec), G9A 5H7, Canada, and Laboratory of Chemistry, Department of Science, Agricultural University of Athens, 75 Iera Odos, 118 55 Athens, Greece

Received: December 7, 2009; Revised Manuscript Received: January 21, 2010

We report the complexation of bovine serum albumin (BSA) with resveratrol, genistein, and curcumin, at physiological conditions, using constant protein concentration and various polyphenol contents. FTIR, CD, and fluorescence spectroscopic methods were used to analyze the ligand binding mode, the binding constant, and the effects of complexation on BSA stability and conformation. Structural analysis showed that polyphenols bind BSA *via* hydrophilic and hydrophobic interactions with the number of bound polyphenol (*n*) being 1.30 for resveratrol−BSA, 1.30 for genisten−BSA, and 1.0 for curcumin−BSA. The polyphenol−BSA binding constants were $K_{Res-BSA} = 2.52(\pm0.5) \times 10^4\ M^{-1}$, $K_{Gen-BSA} = 1.26(\pm0.3) \times 10^4\ M^{-1}$, and $K_{Cur-BSA} = 3.33(\pm0.8) \times 10^4\ M^{-1}$. Polyphenol binding altered BSA conformation with a major reduction of α-helix and an increase in β-sheet and turn structures, indicating a partial protein unfolding.

Introduction

Resveratrol (3,5,4′-trihydroxystilbene) (Scheme 1) is a natural polyphenolic compound produced in plants (e.g., grapes, peanuts, mulberries) in response to injury and fungal attack. Resveratrol can also be found in food products and beverages such as peanut butter, red wine, grape juice, and more recently in dark chocolate and cocoa liquor.[1−3] It has been identified as a potential cardioprotective and chemopreventive agent against chemical carcinogens.[4] It is known to arrest cell cycle at the transition phase from S to G2/M in SW480 human colorectal cells.[5] The OH group at the C-4 position in resveratrol has a major role in antioxidant activity (Scheme 1).[6]

Genistein (4′,5,7-trihydroxy isoflavone) (Scheme 1), present in soybeans and chickpeas, has a wide spectrum of physiological and pharmacological functions. It is known to antagonize human melanoma cell growth at G2/M transition[7,8] and has been found to inhibit H_2O_2/Cu(II) mediated DNA strand breaks acting as a direct scavenger of reactive oxygen species with the OH group at the C-4 position responsible for its antioxidant activity.

Curcumin [(1,7-bis-(4-hydroxy-3-methoxyphenyl)-1,6-heptadiens-3,5-dione)] (Scheme 1) is the main yellow pigment of the powdered rhiome (turmeric) of the herb *Curcuma longa* used for centuries as a spice and food coloring agent.[9] It has also been used to treat diseases such as inflammation, skin wounds, and tumors as traditional medicine.[10] Curcumin exhibits antioxidant activity both *in vivo* and *in vitro.*[11] Apart from its anti-inflammatory, antimicrobial, and antiviral properties, curcumin is considered as a cancer chemopreventive agent.[11,12] However, polyphenols can be transported by serum albumins *in vivo* and thus their interactions with these proteins are of major biological importance.

SCHEME 1: Chemical Structures of Resveratrol, Genistein, and Curcumin

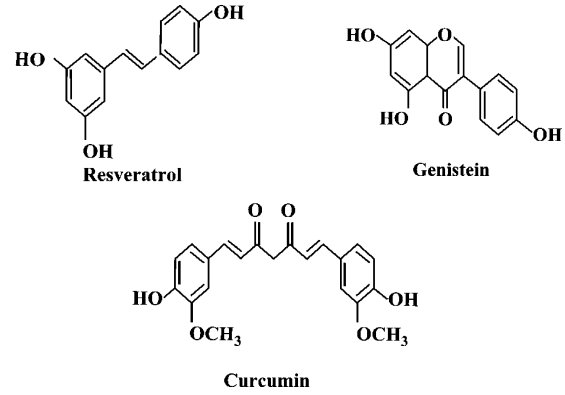

SCHEME 2: Structure of Bovine Serum Albumin with Tryptophan Residues Shown in Green Color

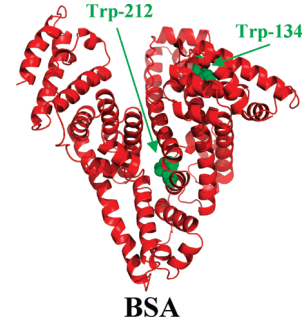

Serum albumins are the major soluble protein constituents of the circulatory system and have many physiological functions.[13] The most important property of this group of proteins is that they serve as transporters for a variety of compounds. BSA (Scheme 2) has been one of the most extensively studied of this group of proteins, particularly because of its structural homology with human serum albumin (HSA). The BSA molecule is made up of three homologous domains (I, II, III) that are divided into nine loops (L1−L9) by 17 disulfide bonds.

† Abbreviations: BSA, bovine serum albumin; HSA, human serum albumin; Res, resveratrol; Gen, genistein; Cur, curcumin; FTIR, Fourier transform infrared spectroscopy; CD, circular dichroism.

* Corresponding author. Fax: 819-376-5084. Phone: 819-376-5011 (ext. 3310). E-mail: tajmirri@uqtr.ca.

‡ Université du Québec à Trois-Rivières.

§ Agricultural University of Athens.

10.1021/jp9115996
Published on Web 02/11/2010

The loops in each domain are made up of a sequence of large−small−large loops forming a triplet. Each domain in turn is the product of two subdomains (IA, IB, etc.). X-ray crystallographic data[14,15] show that the albumin structure is predominantly α-helical with the remaining polypeptide, occurring in turns and in extended or flexible regions between subdomains with no β-sheets. BSA has two tryptophan residues that possess intrinsic fluorescence,[16,17] Trp-134 in the first domain and Trp-212 in the second domain. Trp-212 is located within a hydrophobic binding pocket of the protein, and Trp-134 is located on the surface of the molecule. While there are marked similarities between BSA and HSA in their compositions, HSA has only one tryptophan residue Trp-214, while BSA contains two tryptophans Trp-212 and Trp-134 as fluorphores capable of fluorescence quenching.

Fluorescence quenching is considered as a technique for measuring binding affinities. Fluorescence quenching is the decrease of the quantum yield of fluorescence from a fluorophore induced by a variety of molecular interactions with a quencher molecule.[18] Therefore, it was of interest to use quenching of the intrinsic tryptophan fluorescence of BSA as a tool to study the interaction of polyphenols with BSA in an attempt to characterize the nature of polyphenol−protein complexation.

We report the spectroscopic analysis of BSA complexes with resveratrol, genistein, and curcumin in aqueous solution at physiological conditions, using constant protein concentration and various pigment contents. Structural information regarding polyphenol binding mode and the effect of polyphenol−BSA complexation on the protein stability and secondary structure is reported here.

Experimental Section

Materials. BSA fraction V and resveratrol, genistein, and curcumin were purchased from Sigma Chemical Company and used as supplied. Other chemicals were of reagent grade and used without further purification.

Preparation of Stock Solutions. Bovin serum albumin was dissolved in aqueous solution (40 mg/mL or 0.5 mM) containing 10 mM Tris−HCl buffer (pH 7.4). The protein concentration was determined spectrophotometrically using an extinction coefficient of 36 500 M^{-1} cm^{-1} at 280 nm.[19] Polyphenol solution (1 mM) was first prepared in Tris−HCl/ethanol 50% and then diluted by serial dilution to 0.5, 0.25, and 0.125 mM in Tris−HCl/ethanol 50%. After addition of an equal volume of pigment solution to protein solution, the final ethanol concentration was reduced to 25%. The presence of 25% of ethanol induces no major BSA structural changes according to a recent publication.[20]

FTIR Spectroscopic Measurements. Infrared spectra were recorded on a FTIR spectrometer (Impact 420 model), equipped with a deuterated triglycine sulfate (DTGS) detector and KBr beam splitter, using AgBr windows. A solution of polyphenol was added dropwise to the BSA solution with constant stirring to ensure the formation of homogeneous solution and to have pigment concentrations of 0.125, 0.25, and 0.5 mM with a final protein concentration of 0.25 mM (20 mg/mL). Spectra were collected after 2 h of incubation of BSA with pigment solution at room temperature, using hydrated films. Interferograms were accumulated over the spectral range 4000−600 cm^{-1} with a nominal resolution of 2 cm^{-1} and 100 scans. The difference spectra [(protein solution + polyphenol solution) − (protein solution)] were generated using the water combination mode around 2300 cm^{-1}, as the standard.[21] When producing difference spectra, this band was adjusted to the baseline level, in order to normalize difference spectra.

Analysis of Protein Conformation. Analysis of the secondary structure of BSA and its polyphenol complexes was carried out on the basis of the procedure previously reported.[22] The protein secondary structure is determined from the shape of the amide I band, located around 1660−1650 cm^{-1}. The FTIR spectra were smoothed, and their baselines were corrected automatically using Grams AI software. Thus, the root-mean-square (rms) noise of every spectrum was calculated. By means of the second derivative in the spectral region 1700−1600 cm^{-1}, the major peaks for BSA and the complexes were resolved. The above spectral region was deconvoluted by the curve-fitting method with the Levenberg−Marquadt algorithm and the peaks corresponding to α-helix (1658−1656 cm^{-1}), β-sheet (1640−1610 cm^{-1}), turn (1670−1665 cm^{-1}), random coil (1648−1641 cm^{-1}), and β-antiparallel (1692−1680 cm^{-1}) were adjusted and the area measured with the Gaussian function. The area of all of the component bands assigned to a given conformation were then summed up and divided by the total area.[23,24] The curve-fitting analysis was performed using the GRAMS/AI Version 7.01 software of the Galactic Industries Corporation.

Circular Dichroism. CD spectra of BSA and its pigment complexes were recorded with a Jasco J-720 spectropolarimeter. For measurements in the far-UV region (178−260 nm), a quartz cell with a path length of 0.01 cm was used in nitrogen atmosphere. BSA concentration was kept constant (12.5 μM), while varying each pigment concentration (0.125, 0.25, and 0.5 mM). An accumulation of three scans with a scan speed of 50 nm/min was performed, and data were collected for each nm from 260 to 180 nm. Sample temperature was maintained at 25 °C using a Neslab RTE-111 circulating water bath connected to the water-jacketed quartz cuvettes. Spectra were corrected for buffer signal, and conversion to the Mol CD ($\Delta\varepsilon$) was performed with the Jasco Standard Analysis software. The protein secondary structure was calculated using CDSSTR, which calculates the different assignments of secondary structures by comparison with CD spectra, measured from different proteins for which high quality X-ray diffraction data are available.[25,26] The program CDSSTR is provided in the CDPro software package which is available at the Web site http://lamar.colostate.edu/~sreeram/CDPro.

Fluorescence Spectroscopy. Fluorometric experiments were carried out on a Varian Cary Eclipse. Stock solutions of 1 mM polyphenol in buffer (pH 7.4) were prepared at room temperature (24 ± 1 °C). Various solutions of polyphenol (2−200 μM) were prepared from the above stock solutions by successive dilutions also at 24 ± 1 °C. A solution of BSA (15 μM) in 10 mM Tris−HCl (pH. 7.4) was also prepared at 24 ± 1 °C. The above solutions were kept in the dark and used soon after. Samples containing 2 mL of the above BSA solution and 2 mL of various polyphenol solutions were mixed to obtain a final polyphenol concentration of 1−100 μM with a constant BSA content of 7.5 μM. The fluorescence spectra were recorded at $\lambda_{exc} = 280$ nm and λ_{em} from 287 to 500 nm. The intensity at 340 nm (tryptophan) was used to calculate the binding constant (K) according to literature reports.[27−30]

Molecular Modeling of Bovine Serum Albumin. The structure of BSA was predicted by automated homology modeling using the SWISS-MODEL Workspace from the amino acid sequence NP-851335.[31,32] The structure of free HSA (PDB id: 1AO6, chain A) obtained by X-ray crystallography was used as a template.[33] These two proteins share 78.1% of sequence identity, which is sufficient to obtain reliable sequence align-

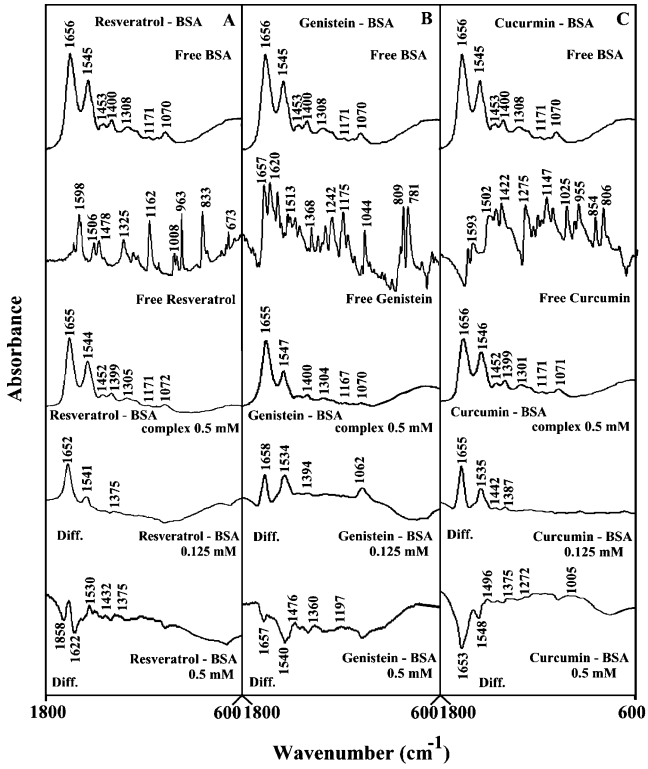

Figure 1. FTIR spectra in the region 1800−600 cm^{-1} of hydrated films (pH 7.4) for free BSA (0.25 mM), A) free resveratrol (1 mM), B), free genistein (1 mM), C), free curcumin (1 mM) and their BSA complexes with difference spectra (diff.) obtained at different polyphenol concentrations (indicated in the figure). The contribution of the polyphenols is subtracted from difference spectra in this region.

ment.[34] Images of the structures were generated using Pymol (DeLano Scientific, Palo Alto, CA). The rmsd between model and template proteins was 0.20 Å for positions of backbone atoms, as calculated with DeepView/Swiss-PdbViewer 4.0.1 (Scheme 2). The quality of the predicted BSA structure was found to be similar to the structure of free HSA used here as a template using structure and model assessment tools of the SWISS-MODEL workspace.

Results and Discussion

FTIR Spectra of Polyphenol−BSA Complexes. The polyphenol−BSA interaction was characterized by infrared spectroscopy and its derivative methods. Since there was no major spectral shifting for the protein amide I band at 1656 cm^{-1} (mainly C═O stretch) and amide II band at 1545 cm^{-1} (C−N stretching coupled with N−H bending modes)[22,35] upon polyphenol interaction, the difference spectra [(protein solution + polyphenol solution) − (protein solution)] were obtained, in order to monitor the intensity variations of these vibrations and the results are shown in Figure 1. Similarly, the infrared self-deconvolution with second derivative resolution enhancement and curve-fitting procedures[22] were used to determine the protein secondary structures in the presence of polyphenol (Figure 2 and Table 1). CD spectroscopy was also used to analyze the protein conformation in the pigment−BSA complexes, and the results are shown in Table 2.

At low polyphenol concentration (0.125 mM), an increase in intensity was observed for the protein amide I at 1656 and amide II at 1545 cm^{-1}, in the difference spectra of the resveratrol−BSA, genistein−BSA, and curcumin−BSA complexes (Figure 1, diff. 0.125 mM). Positive features are observed

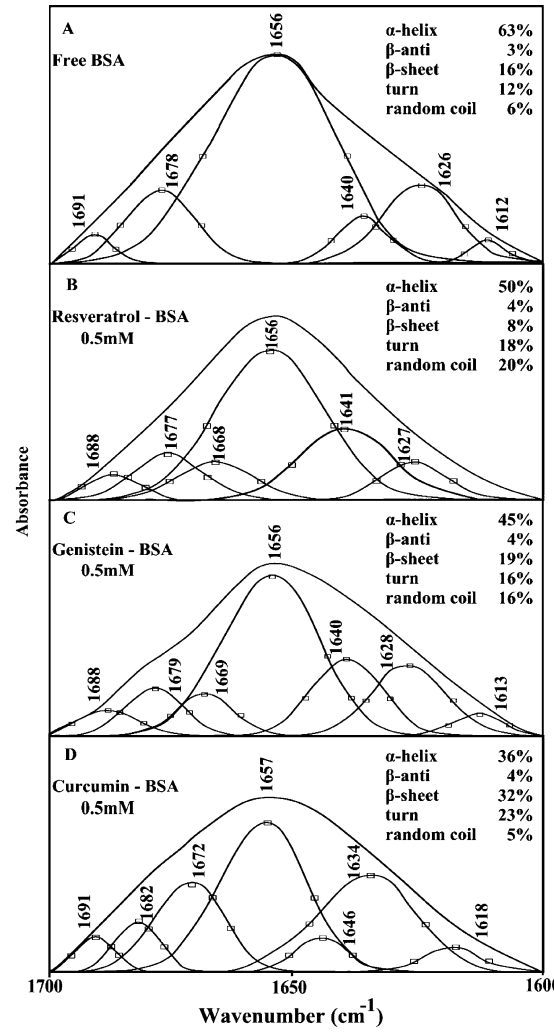

Figure 2. Second derivative resolution enhancement and curve-fitted amide I region (1700−1600 cm^{-1}) for free BSA and its polyphenol adducts with 0.5 mM pigment and 0.25 mM protein concentrations at pH 7.4.

TABLE 1: Secondary Structure Analysis (Infrared Spectra) from the Free BSA and Its Polyphenol Complexes in Hydrated Film at pH 7.4

amide I components (cm^{-1})	free BSA (%), 0.5 mM	resveratrol−BSA (%), 0.5 mM	genistein−BSA (%), 0.5 mM	curcumin−BSA (%), 0.5 mM
1692−1680 β-anti (±1)	3	4	4	4
1680−1660 turn (±2)	12	18	16	23
1660−1650 α-helix (±3)	63	50	45	36
1648−1641 random coil (±1)	6	20	16	5
1640−1610 β-sheet (±2)	16	8	19	32

in the difference spectra for amide I and II bands at 1652 and 1541 cm^{-1} (resveratrol), 1658 and 1534 cm^{-1} (genistein), and 1655 and 1535 cm^{-1} (curcumin) (Figure 1, diff., 0.125 mM). These positive features are related to an increase in intensity of the amide I and amide II bands upon polyphenol complexation. The increase in intensity of the amide I and amide II bands is due to polyphenol binding to protein C═O, C−N, and N−H groups. Additional evidence to support the protein interaction with C−N and N−H groups comes from the shifting of the

TABLE 2: Secondary Structure of BSA Complexes (CD Spectra) with Polyphenols at pH 7.4 Calculated by CDSSTR Software

pigment concentration	α-helix (%) (±3)	β-sheet (%) (±2)	turn (%) (±2)	random (%) (±2)
free BSA (12.5 μM)	62	13	14	11
resveratrol−BSA (0.5 mM)	50	20	16	14
genistein−BSA (0.5 mM)	45	25	18	12
curcumin−BSA (0.5 mM)	39	29	20	12

protein amide A band at 3290 cm^{-1} (N—H stretching mode) in the free BSA to 3285 (resveratrol), 3284 (genistein), and 3283 cm^{-1} (curcumin), upon polyphenol−protein complexation (spectra not shown).

As the polyphenol concentration increased to 0.5 mM, a decrease in intensity of the amide I band was observed with features at 1658 cm^{-1} (resveratrol), 1657 cm^{-1} (genistein), and 1653 cm^{-1} (curcumin) in the difference spectra of polyphenol−BSA complexes (Figure 1, diff, 0.5 mM). The observed decrease in intensity of the amide I band in the spectra of the pigment−protein complexes suggests a major reduction of protein α-helical structure at high polyphenol concentrations. Similar infrared spectral changes were observed for the protein amide I band in several ligand−protein complexes, where major protein conformational changes occurred.[36]

A quantitative analysis of the protein secondary structure for the free BSA and its polyphenol adducts in hydrated films has been carried out, and the results are shown in Figure 2 and Table 1. The free protein was 63% α-helix (1656 cm^{-1}), 16% β-sheet (1626 and 1612 cm^{-1}), 12% turn structure (1678 cm^{-1}), 3% β-antiparallel (1691 cm^{-1}), and 6% random coil (1640 cm^{-1}) (Figure 2A and Table 1). The results are consistent with the spectroscopic studies of bovine serum albumin previously reported.[37,38] Upon polyphenol interaction, a major decrease of α-helix from 63% (free BSA) to 50% (resveratrol−BSA), 45% (genistein−BSA), and 36% (curcumin−BSA) with an increase in β-sheet from 16% (free BSA) to 19% (genistein), and 32% (curcumin) was observed (Figure 2 and Table 1). A similar increase was also observed for the turn structure from 12% (free BSA) to 18% (resveratrol), 16% (genistein), and 23% (curcumin) (Figure 2 and Table 1). These results are consistent with the decrease in the intensity of the protein amide I band discussed above. The major decrease in α-helix structure and increase in β-sheet and turn structures suggest a partial protein unfolding at high polyphenol concentrations.

The conformational changes observed from infrared results for BSA and its pigment complexes are consistent with CD spectroscopic data shown in Table 2. The CD results suggest that free BSA has a high α-helix content of 62%, 13% β-sheet, 14% turn, and 11% random coil (Table 2), consistent with the literature report.[37] Upon polyphenol complexation, major reduction of α-helix was observed from 62% in free BSA to 50% in resveratrol, 45% in genistein, and 39% in curcumin complexes (Table 2). The decrease in α-helix was accompanied by an increase in the β-sheet and turn structures (Table 2). The major reduction of the α-helix with an increase in the β-sheet and turn structures is consistent with the infrared results that showed reduction of α-helix and increase of β-sheet and turn structures due to a partial protein unfolding (Tables 1 and 2).

Hydrophobic Interactions. In order to examine the hydtrophobic contact in the polyphenol−protein complexes, the BSA

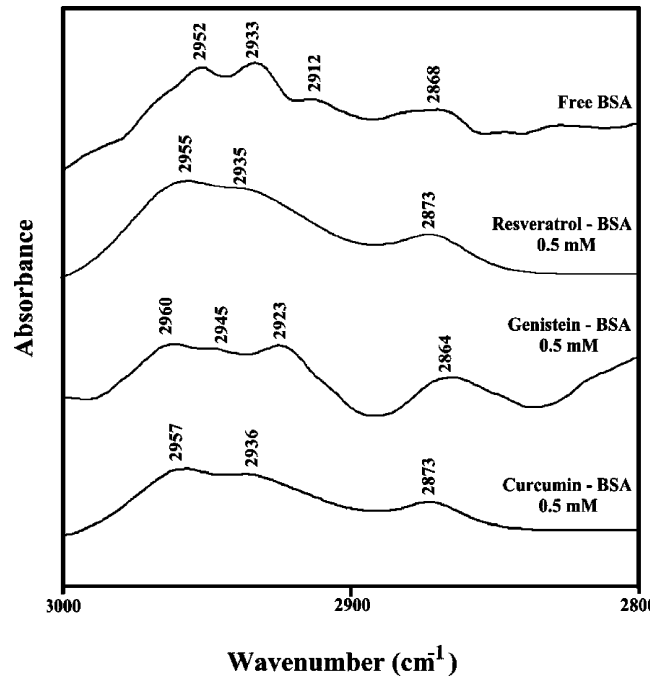

Figure 3. Infrared spectra of protein CH_2 symmetric and antisymmetric stretching vibrations and its polyphenol−BSA complexes in the region 3000−2800 cm^{-1}. The contribution of the CH stretching vibrations of the polyphenolic compounds in the region 3000−2800 cm^{-1} is subtracted.

antisymmetric and symmetric CH_2 stretching vibrations[35] in the region 3000−2800 cm^{-1} were used. The CH_2 bands of the free BSA located at 2952, 2933, 2912, and 2868 cm^{-1} shifted to 2955, 2935, and 2873 cm^{-1} (resveratrol); to 2960, 2945, 2923, and 2864 (genistein), and 2957, 2936, and 2873 cm^{-1} (curcumin), in these pigment−protein complexes (Figure 3). The shifting of the protein antisymmetric and symmetric CH_2 stretching vibrations suggests the presence of hydrophobic interactions *via* polyphenolic rings and hydrophobic pockets in BSA (Figure 3).

Fluorescence Spectra and Stability of Polyphenol−BSA Complexes. BSA has two tryptophan residues that possess intrinsic fluorescence.[16,17] Trp-212 is located within a hydrophobic binding pocket of the protein, and Trp-134 is located on the surface in the hydrophilic region of the molecule (Scheme 2). Tryptophan emission dominates BSA fluorescence spectra in the UV region. When other molecules interact with BSA, tryptophan fluorescence may change depending on the impact of such interaction on the protein conformation.[18] On the assumption that there are (n) substantive binding sites for quencher (Q) on protein (B), the quenching reaction can be shown as follows:

$$nQ + B \leftrightarrow Q_nB \quad (1)$$

The binding constant (K_A) can be calculated as

$$K_A = [Q_nB]/[Q]^n[B] \quad (2)$$

where [Q] and [B] are the quencher and protein concentration, respectively, $[Q_nB]$ is the concentration of non-fluorescent fluorophore−quencher complex, and $[B_0]$ gives the total protein concentration:

$$[Q_nB] = [B_0] - [B] \quad (3)$$

$$K_A = [B_0] - [B]/[Q]^n[B] \quad (4)$$

The fluorescence intensity is proportional to the protein concentration as described:

$$[B]/[B_0] \propto F/F_0 \quad (5)$$

Results from fluorescence measurements can be used to estimate the binding constant of the polyphenol−protein complex. From eq 4,

$$\log[(F_0 - F)/F] = \log K_A + n \log[Q] \quad (6)$$

The accessible fluorophore fraction (f) can be calculated by a modified Stern−Volmer equation:

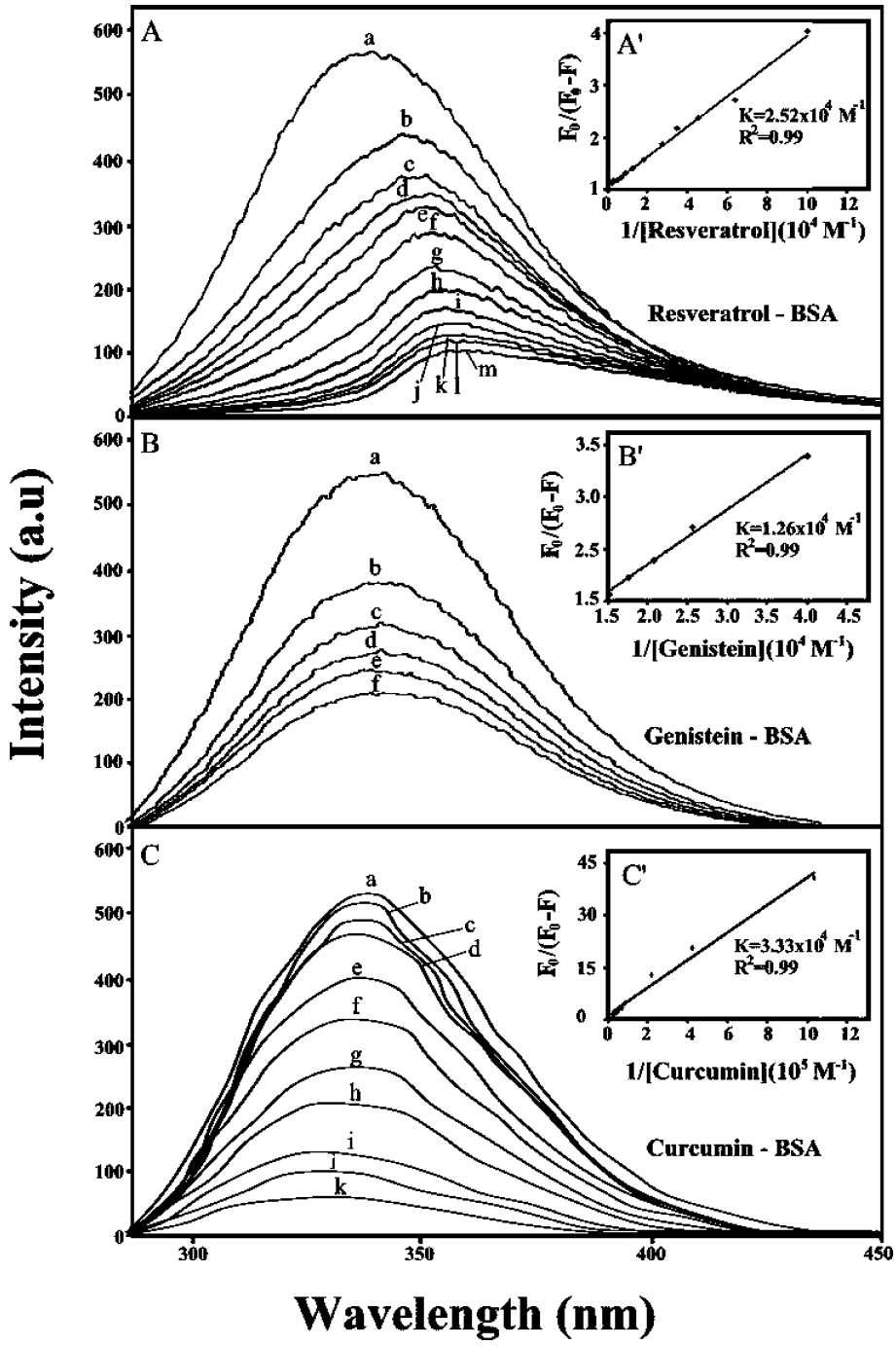

Figure 4. Fluorescence emission spectra of pigment−BSA systems in 10 mM Tris−HCl buffer (pH 7.4) at 25 °C for (A) resveratrol−BSA: (a) free BSA (7.5 μM), (b−m) with resveratrol at 10, 15, 20, 25, 30, 40, 50, 60, 70, 80, 90, and 100 μM; (B) genistein−BSA: (a) free BSA (7.5 μM), (b−f) with genistein at 25, 40, 50, 60, and 70 μM; (C) curcumin−BSA: (a) free BSA (7.5 μM); (b−k) with curcumin at 1, 2.5, 5, 15, 20, 30, 40, 60, 80, and 100 μM. The plot of $F_0/(F_0 - F)$ as a function of 1/pigment concentration with the binding constant K being the ratio of the intercept and the slope for (A′) resveratrol−BSA, (B′) genistein−BSA, and (C′) curcumin−BSA complexes.

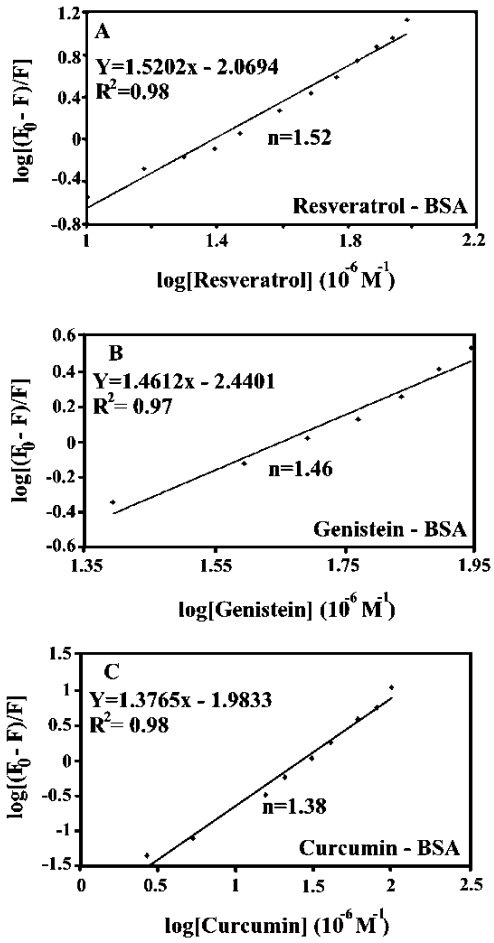

Figure 5. Plot of $\log(F_0 - F)/F$ as a function of log[polyphenol] for calculation of the number of bound polyphenol (n) in polyphenol−BSA complexes.

$$F_0/(F_0 - F) = 1/fK[\mathrm{Q}] + 1/f \quad (7)$$

where F_0 is the initial fluorescence intensity and F is the fluorescence intensity in the presence of quenching agent (or interacting molecule). K is the Stern−Volmer quenching constant, [Q] is the molar concentration of quencher, and f is the fraction of accessible fluorophore to a polar quencher, which indicates the fractional fluorescence contribution of the total emission for an interaction with a hydrophobic quencher.[18] The plot of $F_0/(F_0 - F)$ vs 1/[Q] yields f^{-1} as the intercept on the y axis and $(fK)^{-1}$ as the slope. Thus, the ratio of the ordinate and the slope gives K. The decrease of the fluorescence intensity of BSA is monitored at 340 nm in pigment−BSA systems (Figure 4 shows representative results for each system). The plot of $F_0/(F_0 - F)$ vs 1/[polyphenol] is shown for polyphenol−BSA complexes (Figure 4, A′, B′, and C′ show representative plots). Assuming that the observed changes in fluorescence come from the interaction between polyphenol and BSA, the quenching constant can be taken as the binding constant of the complex formation. The K values given here are averages of four-replicate and six-replicate runs for polyphenol/BSA systems, each run involving several different concentrations of polyphenol (Figure 4). The binding constants obtained were $K_{\mathrm{Res-BSA}} = 2.52(\pm 0.5) \times 10^4\ \mathrm{M}^{-1}$, $K_{\mathrm{Gen-BSA}} = 1.26(\pm 0.3) \times 10^4\ \mathrm{M}^{-1}$, and $K_{\mathrm{Cur-BSA}} = 3.33(\pm 0.8) \times 10^4\ \mathrm{M}^{-1}$ (Figure 4A′−C′). The binding constants calculated for polyphenol−BSA suggest low affinity pigment−BSA binding, compared to the other strong ligand−protein complexes.[39,40] However, lower binding constants (10^4 to $10^3\ \mathrm{M}^{-1}$) were also reported for several other ligand−protein complexes using fluorescence spectroscopic methods.[41−45]

The f values shown in Figure 4 suggest that polyphenol interacts with fluorophore *via* hydrophobic interactions. As a result, we predict that polyphenol binds mainly with the two fluorophores, Trp-212 buried inside and Trp-134 located on the surface of BSA. This argument is based on the fact that the emissions $\lambda_{\max}$ of Trp-212 and Try-134 are at 340 nm (Figure 4), which is the emission region of hidden tryptophan molecules, while fluorescence emission of exposed tryptophan molecule is at higher wavelength (350 nm) due to solvent relaxation.[46−56] The tightening of protein structure through intramolecular interactions, such as hydrogen bonds, seems to bury Trp-212 in a more hydrophobic environment. The change in fluorescence intensity of Trp-212 and Trp-134 in the presence of polyphenol may arise as a direct quenching or as a result of protein conformational changes induced by polyphenol−BSA complexation. The results indicate that polyphenol interactions do not change the emission $\lambda_{\max}$ at 340 nm for genistein and curcumin, whereas a major shifting of this band occurred upon resveratrol−BSA complexation (Figure 4). The lack of spectral shifting observed for the emission band of tryptophan at 340 nm upon genistein and curcumin interaction is indicative of tryptophan molecules not exposed to any change in polarity. However, the major shifting of the emission band at 340−360 nm for the resveratrol−BSA adduct is due to exposed tryptophan (Figure 4A). The observed spectral changes for the emission $\lambda_{\max}$ of quenched tryptophan are due to polyphenol interaction with BSA *via* hydrophobic and hydrophilic regions located inside and on the surface. This argument is consistent with the infrared analysis of protein CH_2 antisymmetric and symmetric stretching vibrations that showed hydrophobic contact in pigment−BSA complexes (Figure 3). Evidence for hydrophilic interaction was discussed in the infrared section (Figure 1). However, the binding mode of resveratrol is somehow different from genistein and curcumin in these polyphenol−BSA complexes. Resveratrol can penetrate inside where Trp-212 is buried and establishes more hydrophobic contact than those of genistein and curcumin. However, such penetration by resveratrol does not alter protein conformation as much as for genistein and curcumin.

The number of polyphenol bound per protein (n) is calculated from $\log[(F_0 - F)/F] = \log K_S + n \log[\text{polyphenol}]$ for the static quenching.[46−52] The linear plot of $\log[(F_0 - F]/F]$ as a function of log[polyphenol] is shown in Figure 5. The n values from the slope of the straight line are 1.52 (resveratrol), 1.46 (genistein), and 1.38 (curcumin) (Figure 5). It seems that more than one molecule of the polyphenols bind BSA, in these pigment−protein complexes (Figure 5).

Comparison between Polyphenol−BSA and Polyphenol−HSA Interactions. Due to the marked structural similarities of BSA and HSA (78.1%), a comparison was made between polyphenol−BSA and polyphenol−HSA complexes. Resveratrol, genisten, and curcumin bind HSA *via* hydrophilic and hydrophobic interactions with overall binding constants of $K_{\mathrm{Res-HSA}} = 2.56 \times 10^5\ \mathrm{M}^{-1}$, $K_{\mathrm{Gen-HSA}} = 2.4 \times 10^4\ \mathrm{M}^{-1}$, and $K_{\mathrm{Cur-HSA}} = 5.5 \times 10^4\ \mathrm{M}^{-1}$ with the order of stability Res > Cur > Gen.[57,58] Polyphenol bindings to BSA were through hydrophilic and hydrophobic interactions with the binding constants of $K_{\mathrm{Res-BSA}} = 2.52 \times 10^4\ \mathrm{M}^{-1}$, $K_{\mathrm{Gen-BSA}} = 1.26 \times 10^4\ \mathrm{M}^{-1}$, and $K_{\mathrm{Cur-BSA}} = 3.33 \times 10^4\ \mathrm{M}^{-1}$. Stronger binding was observed for polyphenol−HSA than polyphenol−BSA complexation. The binding mode of resveratrol−HSA was different from those of genistein−HSA and curcumin−HSA complexes, which induced

a major increase of protein α-helix from 55% (free HSA) to 62% in res-HSA adduct, while genistein and curcumin caused some reduction of protein α-helix to 51% (genistein) and 48% (curcumin) in the polyphenol−HSA complexes.[57,58] However, polyphenol−BSA interaction induced major reduction of protein α-helix from 63% (free BSA) to 50% (resveratrol), 45% (genistein), and 36% (curcumin) (Table 1). This comparison shows larger protein unfolding occurred for BSA than HSA upon polyphenol−protein complexation.

Conclusions. Based on our spectroscopic data, polyphenol binding to BSA occurs *via* hydrophilic and hydrophobic interactions and causes a partial protein unfolding. The affinity of polyphenol−protein complexation is curcumin > resveratrol > genistein with the binding constants of $K_{Res-BSA} = 2.52 \times 10^4\ M^{-1}$, $K_{Gen-BSA} = 1.26 \times 10^4\ M^{-1}$, and $K_{Cur-BSA} = 3.33 \times 10^4\ M^{-1}$. Larger perturbations of protein secondary structure occurred for curcumin > genistein > resveratrol. The pigment−BSA binding site is mainly in the vicinity of Trp-212 and Trp-134 located in the protein domains I and II.

Acknowledgment. This work is supported by a grant from Natural Sciences and Engineering Research Council of Canada (NSERC).

References and Notes

(1) Stervbo, U.; Vang, O.; Bonnesen, C. *Food Chem.* **2007**, *101*, 449–457.
(2) Counet, C.; Callemien, D.; Collin, S. *Food Chem.* **2006**, *98*, 649–657.
(3) PaceAsciak, C. R.; Rounova, O.; Hahn, S. E.; Diamandis, E. P.; Goldberg, D. M. *Clin. Chim. Acta* **1996**, *246*, 163–182.
(4) Cao, X.; Xu, Y. X.; Divine, G.; Janakiraman, N.; Chapman, R. A.; Gautam, S. C. *J. Nutr.* **2002**, *132*, 2076–2081.
(5) Delmas, D.; Passilly-Degrace, P.; Jannin, B.; Malik, M. C.; Latruffe, N. *Int. J. Mol. Med.* **2002**, *10*, 193–199.
(6) Ahmad, A.; Asad, S. F.; Singh, S.; Hadi, S. M. *Cancer Lett.* **2000**, *154*, 29–37.
(7) Matsukawa, Y.; Marui, N.; Sakai, T.; Satomi, Y.; Yoshida, M.; Matsumoto, K.; Nishino, H.; Aoike, A. *Cancer Res.* **1993**, *53*, 1328–1331.
(8) Win, W.; Cao, Z.; Peng, X.; Trush, M. A.; Li, Y. *Mutat. Res.* **2002**, *513*, 113–120.
(9) Salvioli, S.; Sikora, E.; Cooper, E. L.; Franceschi, C. *Evid. Based Complement. Alternat. Med.* **2007**, *4*, 181–190.
(10) Maheshwari, R. K.; Singh, A. K.; Gaddipati, J.; Srimal, R. C. *Life Sci.* **2006**, *78*, 2081–2087.
(11) Kunnumakkara, A. B.; Guha, S.; Krishnan, S.; Diagaradjane, P.; Gelovani, J.; Aggarwal, B. B. *Cancer Res.* **2007**, *67*, 3853–3861.
(12) Rao, C. V.; Rivenson, A.; Simi, B.; Reddy, B. S. *Cancer Res.* **1995**, *55*, 259–266.
(13) Carter, D. C.; Ho, J. X. *Adv. Protein Chem.* **1994**, *45*, 153–203.
(14) Peters. T. *All about albumin. Biochemistry, Genetics and Medical Applications*; Academic Press: San Diego, CA, 1996.
(15) He, X. M.; Carter, D. C. *Nature* **1992**, *358*, 209–215.
(16) Peters, T. *Adv. Protein Chem.* **1985**, *37*, 161–245.
(17) Tayeh, N.; Rungassamy, T.; Albani, J. R. *J. Pharm. Biomed. Anal.* **2009**, *50*, 107–116.
(18) Lakowicz, J. R. In *Principles of Fluorescence Spectroscopy*, 2nd ed.; Kluwer/Plenum: New York, 1999.
(19) Painter, L.; Harding, M. M.; Beeby, P. J. *J. Chem. Soc., Perkin Trans.* **1998**, *18*, 3041–3044.
(20) Lin, S. Y.; Li, M. J.; Wei, Y. S. *Spectrochim. Acta, Part A* **2004**, *60*, 3107–3111.
(21) Dousseau, F.; Therrien, M.; Pezolet, M. *Appl. Spectrosc.* **1989**, *43*, 538–542.
(22) Byler, D. M.; Susi, H. *Biopolymers* **1986**, *25*, 469–487.
(23) Beauchemin, R.; N' soukpoe-Kossi, C. N.; Thomas, T. J.; Thomas, T.; Carpentier, R.; Tajmir-Riahi, H. A. *Biomacromolecules* **2007**, *8*, 3177–3183.
(24) Ahmed, A.; Tajmir-Riahi, H. A.; Carpentier, R. *FEBS Lett.* **1995**, *363*, 65–68.
(25) Johnson, W. C. *Proteins: Struct., Funct., Genet.* **1999**, *35*, 307–312.
(26) Sreerama, N.; Woddy, R. W. *Anal. Biochem.* **2000**, *287*, 252–260.
(27) Tang, J.; Qi, S.; Chen, X. *J. Mol. Struct.* **2005**, *779*, 87–95.
(28) Bi, S.; Ding, L.; Tian, Y.; Song, D.; Zhou, X.; Liu, X.; Zhang, H. *J. Mol. Struct.* **2005**, *703*, 37–45.
(29) He, W.; Li, Y.; Xue, C.; Hu, Z.; Chen, X.; Sheng, F. *Bioorg. Med. Chem.* **2005**, *13*, 1837–1845.
(30) Dufour, C.; Dangles, O. *Biochim. Biophys. Acta* **2005**, *1721*, 164–173.
(31) Arnold, K.; Bordoli, A. K.; Kopp, L.; Schwede, T. *Bioinformatics* **2006**, *22*, 195–201.
(32) Rost, B. *Protein Eng.* **1999**, *12*, 85–94.
(33) Sugio, S.; Kashima, A.; Mochizuki, S.; Noda, M.; Kobayashi, K. *Protein Eng.* **1999**, *12*, 439–446.
(34) Schwede, T.; Kopp, J.; Guex, N.; Peitsch, M. C. *Nucleic Acids Res.* **2003**, *31*, 3381–3385.
(35) Krimm, S.; Bandekar, J. *Adv. Protein Chem.* **1986**, *38*, 181–364.
(36) Ahmed Ouameur, A.; Diamantoglou, S.; Sedaghat-Herati, M. R.; Nafisi, Sh.; Carpentier, R.; Tajmir-Riahi, H. A. *Cell Biochem. Biophys.* **2006**, *45*, 203–214.
(37) Tian, J.; Liu, J.; Hu, Z.; Chen, X. *Am. J. Immunol* **2005**, *1*, 21–23.
(38) Grdadolnik, J. *Acta Chim. Slov.* **2003**, *50*, 777–788.
(39) Kragh-Hansen, U. *Dan. Med. Bull.* **1990**, *37*, 57–84.
(40) Kratochwil, N. A.; Huber, W.; Muller, F.; Kansy, M.; Gerber, P. R. *Biochem. Pharmacol.* **2002**, *64*, 1355–1374.
(41) N'soukpoé-Kossi, C. N.; Sedaghat-Herati, M. R.; Ragi, C.; Hotchandani, S.; Tajmir-Riahi, H. A. *Int. J. Biol. Macromol.* **2007**, *40*, 484–490.
(42) Liu, J.; Tian, J.; Hu, Z.; Chen, X. *Biopolymers* **2004**, *73*, 443–450.
(43) Dockal, M.; Chang, C.; Carter, D. C.; Ruker, F. *J. Biol. Chem.* **2000**, *275*, 3042–3050.
(44) Liang, L.; Tajmir-Riahi, H. A.; Subirade, M. *Biomacromolecules* **2008**, *9*, 50–55.
(45) Sulkowska, A. *J. Mol. Struct.* **2002**, *614*, 227–232.
(46) Ward, L. D. *Methods Enzymol.* **1995**, *117*, 400–404.
(47) Huang, B. X.; Dass, C.; Kim, Y.-H. *Biochem. J.* **2005**, *387*, 695–702.
(48) Eftink, M. R.; Ghiron, C. A. *Anal. Biochem.* **1981**, *114*, 199–227.
(49) Jiang, C. Q.; Gao, M. X.; He, J. X. *Anal. Chim. Acta* **2002**, *452*, 185–189.
(50) Jiang, M.; Xie, M. X.; Zheng, D.; Liu, Y.; Li, X. Y.; Chen, X. *J. Mol. Struct.* **2004**, *692*, 71–80.
(51) Charbonneau, D.; Beauregard, M.; Tajmir-Riahi, H. A. *J. Phys. Chem. B* **2009**, *113*, 1777–1784.
(52) Froehlich, E.; Mandeville, J. S.; Jennings, C. J.; Sedaghat-Herati, R.; Tajmir- Riahi, H. A. *J. Phys. Chem. B* **2009**, *113*, 6986–6993.
(53) Jiang, X. Y.; Li, W. X.; Cao, H. *J. Solution Chem.* **2008**, *37*, 1609–1623.
(54) Cao, S.; Li, H.; Chen, T.; Chen, J. *J. Solution Chem.* **2009**, *38*, 1520–1527.
(55) Barik, A.; Priyadarsini, K. L.; Mohan, H. *Photochem. Photobiol.* **2003**, *77*, 597–603.
(56) Mohammadi, F.; Bordbar, A. K.; Divsalar, A.; Mohammadi, K.; Saboury, A. A. *Protein J.* **2009**, *28*, 117–123.
(57) N' soukpoé-Kossi, C. N.; St-Louis, C.; Beauregard, M.; Subirade, M.; Carpentier, R.; Hotchandani, S.; Tajmir-Riahi, H. A. *J. Biomol. Struct. Dyn.* **2006**, *24*, 277–283.
(58) Mandeville, J. S.; Froehlich, E.; Tajmir-Riahi, H. A. *J. Pharm. Biomed. Anal.* **2009**, *49*, 468–474.

JP9115996